Physica A 391 (2012) 343–361

Contents lists available at SciVerse ScienceDirect

Physica A

journal homepage: www.elsevier.com/locate/physa

Community structure in the United Nations General Assembly

Kevin T. Macon [a,b], Peter J. Mucha [a,c,*], Mason A. Porter [d,e]

[a] *Carolina Center for Interdisciplinary Applied Mathematics, Department of Mathematics, University of North Carolina, Chapel Hill, NC 27599-3250, USA*

[b] *Department of Physics, Louisiana State University, Baton Rouge, LA 70803, USA*

[c] *Institute for Advanced Materials, Nanoscience & Technology, University of North Carolina, Chapel Hill, NC 27599, USA*

[d] *Oxford Centre for Industrial and Applied Mathematics, Mathematical Institute, University of Oxford, OX1 3LB, UK*

[e] *CABDyN Complexity Centre, University of Oxford, Oxford OX1 1HP, UK*

ARTICLE INFO

Article history:
Received 19 October 2010
Received in revised form 22 April 2011
Available online 26 June 2011

Keywords:
Networks
Community structure
Modularity
Political networks
Voting networks

ABSTRACT

We study the community structure of networks representing voting on resolutions in the United Nations General Assembly. We construct networks from the voting records of the separate annual sessions between 1946 and 2008 in three different ways: (1) by considering voting similarities as weighted unipartite networks; (2) by considering voting similarities as weighted, signed unipartite networks; and (3) by examining signed bipartite networks in which countries are connected to resolutions. For each formulation, we detect communities by optimizing network modularity using an appropriate null model. We compare and contrast the results that we obtain for these three different network representations. We thereby illustrate the need to consider multiple resolution parameters and explore the effectiveness of each network representation for identifying voting groups amidst the large amount of agreement typical in General Assembly votes.

1. Introduction

The study of networks has a long history in both the mathematical and social sciences [1], and recent investigations have underscored their vibrant interdisciplinary applications and development [2–7]. The large-scale organization of real-world networks typically includes coexisting modular (horizontal) and hierarchical (vertical) organizational structures. Various attempts to interpret such organization have included the computational identification of structural modules called *communities* [8–10], which are obtained by finding groups of nodes such that there are more (or a denser collection of) connections between pairs of nodes in the same group than there are between pairs of nodes assigned to different groups. In principle, communities are not merely structural modules but can have functional importance in network processes. For example, communities in social networks ("cohesive groups" [11]) might correspond to circles of friends or business associates, communities in the World Wide Web might encompass pages on closely related topics, and some communities in biological networks have been shown to be related to functional modules [12,13].

As discussed at length in two recent review articles [8,9] and in references therein, the classes of techniques available to detect communities are both voluminous and diverse. They include hierarchical clustering methods such as single linkage clustering, centrality-based methods, local methods, optimization of quality functions such as modularity and similar quantities, spectral partitioning, likelihood-based methods, and more. Investigations of network community structure have been remarkably successful on benchmark examples [8,14,15] and have led to interesting insights in several

* Corresponding author at: Carolina Center for Interdisciplinary Applied Mathematics, Department of Mathematics, University of North Carolina, Chapel Hill, NC 27599-3250, USA.

E-mail address: mucha@unc.edu (P.J. Mucha).

0378-4371/$ – see front matter
doi:10.1016/j.physa.2011.06.030

applications, including the role of college football conferences [16] in affecting algorithmic rankings [17]; committee assignments [18–20], legislation cosponsorship [21], and voting blocs [22] in the US Congress; the examination of functional groups in metabolic [12] and protein interaction [13] networks; the study of ethnic preferences in school friendship networks [23]; the organization of online social networks [24,25], and the study of social structures in mobile-phone conversation networks [26].

With the newfound wealth of longitudinal data sets on various types of human activity patterns, it has become possible to investigate the temporal dynamics of communities, and this issue has started to attract an increasing amount of attention [26–30]. It is also potentially useful to study community structure in similarity and correlation networks [31], such as those determined by common voting or legislation-cosponsorship patterns [21,22], alliances and disputes among nations [32], or more general coupled time series [28,29]. In such cases, one is faced with numerous choices for how to actually construct the network from the original data – an important issue that has received surprisingly little attention. (An old discussion of some of the available methods is presented in Ref. [33].) In the present paper, we focus on this network construction issue by examining the community structure of networks defined in different ways from roll-call voting patterns in the United Nations General Assembly (UNGA).

The primary goal of this paper is to conduct a comparative investigation of different ways to turn voting data (and similar relational data) into network representations in order to use community detection tools. Community detection can then be used to complement existing approaches such as multidimensional scaling and other data clustering techniques [34,35]. As we discuss in detail below, there are many ways to turn voting data into networks. In this paper, we will compare three ways of doing so using roll-call voting in the UNGA as an illustrative example. For each network representation, we will examine community structure in the UNGA and how it changes over time, and we will compare the results that we obtain using each network representation. Studying community structure entails partitioning a network, and it might be helpful to do so at different network scales [8,9]. We consider different scales using resolution parameters and identify results that are robust with respect to different choices of such parameters.

As discussed in a recent review [36], network analysis has led to interesting insights in the field of international relations – just as it has in numerous other fields in the social, physical, biological, and information sciences [1,3,4,7]. For example, a networks perspective has proven to be important for political studies of social balance [37–39]. Additionally, elements of the Correlates of War (CoW) data [40,41] have been studied using network methods [32,42], and we expect that other available data can also be studied insightfully. Previous studies of UNGA roll-call data have been successful at grouping countries using NOMINATE scores, which assign ideological coordinates to voting members and can be used to introduce partitions in policy space [34,43]. Empirical investigation of UNGA voting behavior has become readily accessible due to Voeten's organization of the UNGA voting data [44]. Voeten analyzed this data using NOMINATE scores to study Cold War and Post-Cold-War voting behavior [43]. Lloyd applied network analysis and correspondence analysis to similar data to show that the so-called ''Clash of Civilizations'' does not occur along civilizational lines (as one might have expected from its name) but rather via a North–South division that arises from economic differences; Lloyd concluded that this division has resulted in varying levels of support for human-rights treaties [45]. Motivated by the previously demonstrated utility of studying community structure in network representations of voting data [22] and legislation cosponsorship data [21] for the United States Congress, we investigate in this paper the community structure of network representations of the UNGA (based on the patterns of roll-call voting on resolutions) to see if such methodologies can help to identify and understand international voting blocs.

The rest of this paper is organized as follows. In Section 2, we give a brief introduction to the United Nations General Assembly voting data and discuss the different ways that we will represent this data in the form of networks. In particular, we construct (1) weighted networks defined by the numbers of voting agreements between pairs of countries; (2) weighted, signed networks in which we separately consider voting agreements and disagreements between countries; and (3) signed bipartite networks between countries and resolutions that directly indicate yes ($+1$) and no (-1) votes. In Section 3, we briefly review community detection via optimization of modularity and its generalizations, and we emphasize the use of appropriate null models with resolution parameters for each of the three network representations that we consider. We then investigate community structure in the UNGA using each of these three formulations and compare our three sets of results. In Section 4, we study the set of resolutions in each session using voting agreements and use our computations to identify historical trends and changes in the UNGA's community structure. We then discuss case studies by going into further detail in one session from each of three different periods in the UNGA's history. We investigate these three sessions (the 11th, 36th, and 58th Sessions) in terms of voting agreements and disagreements in Section 5 and as bipartite networks with positive and negative edges in Section 6. We close with concluding observations in Section 7.

2. Network representations of UNGA voting data

Unlike the other component bodies of the United Nations (UN), the United Nations General Assembly (UNGA) provides equal representation to all member nations [46]. Each nation gets one vote, and UNGA representatives can debate international issues and non-binding resolutions. In recent years, this setting has motivated collaboration among developing countries to create a ''North–South'' division. However, it is unclear how applicable this grouping is in other settings or how cohesive it is on individual issues [43,45,47]. The voting record of the UNGA thereby provides an interesting application for the investigation of network community structure. The UNGA roll call also provides a useful setting for testing the effects

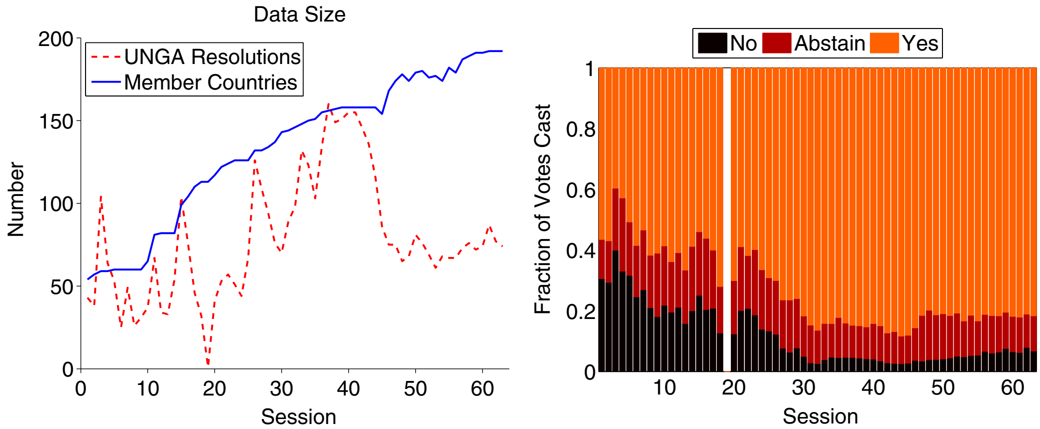

Fig. 1. (Color online) (Left) Numbers of countries (blue) and resolutions (red) in each annual United Nations General Assembly session during 1946–2008. (Session 1 occurred in 1946, etc.) (Right) Fractions of non-unanimous votes cast in each annual session in favor of a resolution (''yes''), against a resolution (''no''), and abstaining.

of different network representations of data for determining voting blocs, in part because one must pay particularly close attention to the baseline level of agreement that is typical in UNGA resolutions that reach a recorded vote. This baseline tendency toward agreement in the data makes the UNGA roll call different from, e.g., studies of roll-call voting and legislation cosponsorship in the United States Congress [21,22,34,48,49].

The UNGA was founded in 1946. As indicated in Fig. 1, the number of member countries has increased steadily since then, but the number of recorded votes has varied from session to session. In this study, we consider every annual session from 1946 to 2008 except for the 19th session (1964), which we exclude because voting occurred on only one resolution in that session. We removed unanimous votes from the data, as they do not provide information about the network structure of voting agreements and disagreements between countries. We note the large amount of agreement in UNGA voting illustrated in the right panel of Fig. 1, indicating the large fraction of ''yes'' votes among the non-unanimous votes that were cast. Importantly, we do keep all votes that are not 100% unanimous, so a significant majority of the remaining votes are still ''yes'' votes. This bias toward agreement skews the simplest measures of voting similarity, so an important area of investigation in the present paper is the consideration of such bias.

Within each session, we determine edge weights between pairs of countries using a measure of the level of their voting agreement. For example, Gartzke's ''The Affinity of Nations'' data set [50] uses a well-known (in the international-relations literature) diagnostic called ''S'' to measure the relative similarity between UNGA votes (the quantity S first converts the voting information to column vectors and then calculates a similarity score between each pair of vectors), with different calculations depending on whether one includes or omits abstentions [51,52]. Assigning numerical values to the types of possible votes – yes, no, abstain, and absent – requires choosing arbitrary relative magnitudes and spacings between these values. For instance, one might assign ± 1 to yes/no votes and choose some intermediate value for abstentions and absences. In doing this, one also must employ some argument as to whether an abstention should be interpreted as closer to a yes or to a no vote. (See the discussions in Refs. [33,43].) Contingency-table statistics also provide a possible way to measure the agreement between voting countries. They avoid the use of a numerical scale but instead require one to assume an expected distribution of votes [33,53].

Motivated by Lijphart's Index of Agreement [33], we define a unipartite network of voting similarities in which the strength of connection between a pair of countries is given by the number of agreements on resolutions (yes–yes, no–no, or abstain–abstain). To avoid assigning artificially high agreement scores to countries with low attendance, we do not normalize by the number of times both countries were present and voting. (This contrasts with the norm when studying voting in legislative networks such as the United States Congress [18,22,34].) One might instead uniformly normalize counts of agreement by the total number of votes in a session, so that an edge of unit strength indicates perfect agreement on all resolutions in a session. However, detecting communities on voting agreement networks when using such a constant intra-session normalization is equivalent to detecting communities on such networks without the normalization. We therefore use the direct count of agreements as the weight of connections in the UN voting agreement networks. We denote the (weighted, unipartite) adjacency matrix of such a network by A^+_{ij}, and we ignore the artificial self-edges imposed by this definition of voting similarity by setting all diagonal entries equal to zero. This is frequently done for correlation networks and is a standard procedure when studying voting similarities [22,28,29,54].

In contrast to a recent study of Congressional roll-call networks [22], the preponderance of ''yes'' votes in the UNGA (see Fig. 1) leads to a wealth of large weights in the voting agreement adjacency matrices A^+_{ij}, and many of these weights are close to the total number of votes in the session. In this environment of significant agreement in voting results, it is unclear how one should best treat abstentions without additional information that details the causes for each such vote. In particular, the relative weight of disagreement between two countries in a yes–abstain pair of votes on a given resolution should presumably be treated differently from that in a yes–no pair or in an abstain–no pair. In order to include the possibility of treating some of these forms of disagreement differently, we count the occasions of direct yes–no disagreement between two countries in the elements of the (symmetric) matrix A^-_{ij} to supplement the (also symmetric) A^+_{ij} agreement matrix. As we discuss in more detail in Section 3, this will entail performing community detection on signed adjacency matrices.

Finally, to ensure that we are not inappropriately discarding too much information about the particular resolutions on which countries vote in agreement (or on yes–no disagreement), we will detect communities in a third class of networks. Each such network (one per UNGA session) consists of a signed bipartite (two-mode) network of countries voting in favor of or against individual resolutions. That is, for each session, we will consider the signed adjacency matrix $\mathbf{V}$ encoding a bipartite network between countries and resolutions. Taking abstentions as zero-valued entries in the absence of other information, we define the matrix elements by

$$V_{ij} = \begin{cases} 1, & \text{if country } i \text{ voted yes on resolution } j, \\ -1, & \text{if country } i \text{ voted no on resolution } j, \\ 0, & \text{otherwise (absences and abstentions).} \end{cases} \quad (1)$$

A pair of countries that both vote in favor of a proposed resolution constitutes some actual agreement between those countries on the resolution (though, of course, such agreement can arise due to various reasons, such as compromise), whereas there might be multiple reasons for two countries to both vote against a resolution [33]. Importantly, community detection on the signed bipartite network representation respects and quantifies this distinction. Countries are more likely to have positive edges to resolutions (i.e., yes votes) within their community and are therefore more likely to be grouped with other countries that vote in favor of many of the same resolutions. In contrast, common votes against a resolution only discourage the placement of the involved no-voting countries in the community containing that resolution.

By investigating community structure using each of these three representations – the $\mathbf{A}^+$ network of agreements alone, the $\mathbf{A}^+$ agreement network together with the $\mathbf{A}^-$ disagreement network, and the underlying bipartite network $\mathbf{V}$ of votes on resolutions – we aim for a more complete picture of the communities present in the UNGA roll call than any one network representation might uncover by itself. More generally, comparing and contrasting these approaches should provide valuable insight about the network treatment of voting and correlation data.

3. Community detection by optimization of generalized modularity

We detect communities by optimizing the quality function known as modularity [55–57], and we also consider some of its generalizations. (Numerous other graph partitioning methods can of course be employed [8,9].) We take the partition with the highest quality value that we can obtain from among three computational heuristics – spectral bipartitioning [57,58], spectral tripartitioning [59], and the locally greedy "Louvain" method [60] – which we subsequently follow in each case by Kernighan–Lin node-swapping steps [57,61] in order to find a partition of the network that has an even higher value of the quality function. Of course, other heuristics (including other greedy methods, extremal optimization, and simulated annealing) can also be employed [8,9,15]. Because modularity (and any similar quality function) has a complex energy landscape that is expected to include a large number of good local optima, one must take care in interpreting results when using it to study the community structure of real networks [62]. Additionally, modularity optimization has a resolution limit [63], so it is important to include resolution parameters to investigate community structure at multiple scales. Exploring the resolution parameter space in each type of network representation is a major focus of the present investigation.

In detecting communities by optimizing modularity (or its generalizations), one partitions a network so that the total strength of intra-community edges is optimized relative to a baseline expectation indicated by an appropriate null model. The quality Q of a partition of the network is a function of the modularity matrix $\mathbf{B} = \mathbf{A} - \gamma\mathbf{P}$, where the adjacency matrix $\mathbf{A}$ encodes the network, the matrix $\mathbf{P}$ encodes the null model, and incorporating a resolution parameter γ allows one to identify communities at different scales [8,9,64]. The quality is given by

$$Q = \sum_{i,j} B_{ij}\delta(c_i, c_j), \quad (2)$$

where $\delta(c_i, c_j)$ equals 1 if i and j have been assigned to the same community and 0 if they have been assigned to different communities. (The community index c_k identifies the community to which node k has been assigned.) Finding the community assignments that maximize Q is an NP-hard problem that requires the use of computational heuristics to obtain a good local optimum [8,9,65]. Importantly, one must select a null model $\mathbf{P}$ that is appropriate for the network under consideration. In particular, we need to use a different null model for each of the three different network representations of UNGA voting that we consider (which, we recall, are the unipartite network of agreements between countries, the unipartite signed network of agreements and disagreements between countries, and the bipartite signed network of yes/no votes by countries on resolutions). After selecting a null model appropriate to a particular network representation, we consider different values of resolution parameters in order to identify communities that persist robustly for a range of resolution parameter values [66].

The unipartite network of agreements, encoded by $\mathbf{A} = \mathbf{A}^+$, is the simplest case to consider. One can employ the standard null model for modularity [56], which is given by $P_{ij} = k_i k_j/(2m)$, where $k_i = \sum_j A_{ij}$ is the strength of node i and $2m = \sum_i k_i = \sum_{ij} A_{ij}$ is the sum of all node strengths. The elements of the modularity matrix are then

$$B_{ij} = \frac{1}{2m}\left(A_{ij} - \gamma \frac{k_i k_j}{2m}\right). \tag{3}$$

When $\gamma = 1$, Eq. (3) reduces to the standard definition of modularity [9,56]. The standard null model for modularity gives the expected edge weights in an unsigned unipartite random graph with independent edges, conditional on having the same expected node strengths as those in the observed network. The standard null model is clearly inappropriate for signed networks and bipartite networks, so other null models must be used instead. In the signed case, the standard null model ignores the potentially important distinction between agreements and disagreements. In the bipartite case, an appropriate null model must respect the constraint that each edge connects nodes of two different types.

Graphs with signed edges can be used to study social networks with both sympathetic (positive) and antagonistic (negative) interactions [67]. This is potentially relevant, for example, for investigations of social balance [68]. A recent paper introduced a generalization of modularity for signed networks and used it to study a network of international alliances and disputes [32]. In our consideration of signed networks, we include the $\mathbf{A}^-$ representation of yes–no disagreements between countries in addition to the $\mathbf{A}^+$ network of agreements. Recall that the absence of agreements indicated in $\mathbf{A}^+$ might include unpaired abstentions or yes–no disagreement, but we include only the latter of these in the specification of $\mathbf{A}^-$ (with such disagreements encoded as $A^-_{ij} > 0$ elements), providing an opportunity to weigh their effects more heavily. Using the signed null model developed in Ref. [32], the modularity matrix becomes

$$B_{ij} = \frac{1}{2m^+ + 2m^-}\left(A^+_{ij} - A^-_{ij} - \gamma \frac{k^+_i k^+_j}{2m^+} + \lambda \frac{k^-_i k^-_j}{2m^-}\right), \tag{4}$$

where $k^\pm_i = \sum_j A^\pm_{ij}$ are the signed strengths for node i and $2m^\pm = \sum_i k^\pm_i = \sum_{ij} A^\pm_{ij}$ are the corresponding total edge weights of the network's two kinds of edges. By using separate resolution parameters for agreements and disagreements, one can investigate and separately examine the effects of these two different types of connections on the community structure. In particular, the resolution parameters separately control the importances of the two types of edges in determining the sizes of the communities (see, e.g., the Laplacian-dynamics interpretation of this signed null model in Ref. [30]).

The extent to which a signed network is socially balanced is strongly related to its community structure [1,68]. In particular, if a network is perfectly socially balanced (in the strong form, so that a triad of nodes with positive edges is considered to be balanced and a triad of nodes with negative edges is considered to be unbalanced [68,69]), then the communities that one finds for $\gamma = \lambda = 0$ in (4) themselves form a socially balanced partition of the network, as all antagonistic interactions (i.e., negative edges) occur between pairs of nodes assigned to different communities. That is, all intra-community edges are non-negative in this extreme scenario. In the presence of incomplete social balance in the network, the communities that one finds for signed networks seek to appropriately optimize the relative numbers of positive and negative edges, connecting the "modern" consideration of community detection to the "classical" one of social balance.

To detect communities in each signed bipartite voting matrix $\mathbf{V}$, we need to generalize the bipartite modularity of Ref. [70] to incorporate both positive and negative edges. A bipartite network consists of two types of nodes – countries and resolutions – and each edge connects a node of one type to a node of the other. The matrix $\mathbf{V}$ encodes connections between countries and resolutions. After ordering the nodes according to type (with the convention that all countries are listed before the resolutions), the corresponding modularity matrix $\mathbf{B}$ in bipartite form consists of off-diagonal blocks:

$$\mathbf{B} = \begin{bmatrix} \mathbf{0} & \tilde{\mathbf{B}} \\ \tilde{\mathbf{B}}^{\mathbf{T}} & \mathbf{0} \end{bmatrix}. \tag{5}$$

Recalling our definition of $\mathbf{V}$ with elements $\{0, \pm 1\}$ encoding votes, the non-zero components of $\mathbf{B}$ then become

$$\tilde{B}_{ij} = V_{ij} - \gamma \frac{k^+_i d^+_j}{2m^+} + \lambda \frac{k^-_i d^-_j}{2m^-}, \tag{6}$$

where $k^\pm_i$ and $d^\pm_j$, respectively, denote the positive and negative degrees (total yes and no votes, respectively) for country i and for resolution j, and $2m^\pm = \sum_i k^\pm_i = \sum_j d^\pm_j$ gives the total number of positive [$(+)$ superscript] and negative [$(-)$ superscript] connections in this network representation [71].

Now that we have described the three network representations of the UNGA roll call that we will consider, we are faced with the dilemma of setting values for the resolution parameters γ and λ. Given some theoretical justification for expected or desired group sizes, one might reasonably study the partitions that one obtains for specific values of the resolution parameters. In the absence of any such additional information, we will instead explore the space of possible resolution parameter values. In doing so, we will focus on communities that appear robustly across a range of different values.

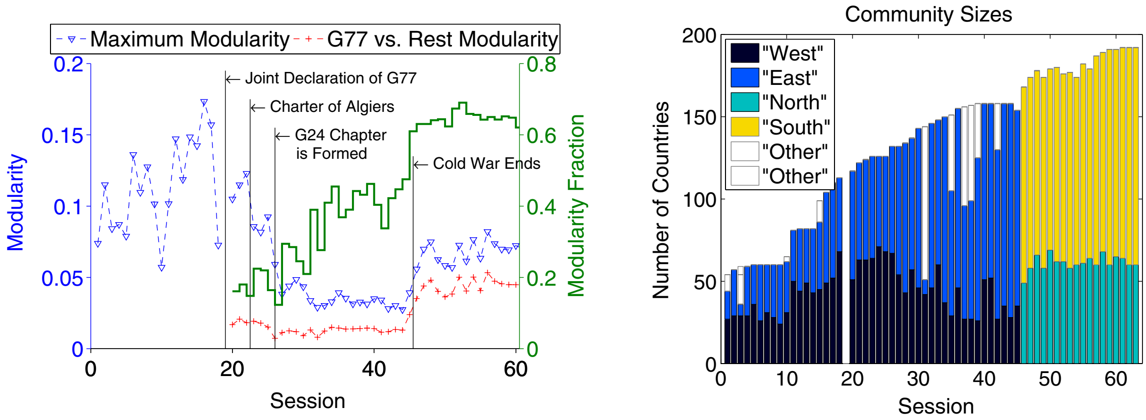

Fig. 2. (Color online) (Left) Maximum modularity obtained by partitioning the (unipartite) voting similarity network of each session. For comparison, we also show the modularity of the partition into G77 and non-G77 countries, revealing the increasing fraction over time (solid curve) of modularity that can be explained by this division of the network. Observe in particular the sharp increase after the end of the Cold War. (Right) Communities identified in each UNGA session using the network of voting similarities. We labeled the dominant countries geographically in each session by tracking the identities of specific countries (e.g., the United Kingdom is typically assigned to the West in every session during the Cold War and to the North group after the Cold War). We list the countries assigned to the North and South communities in Tables 1 and 2, respectively.

Table 1
39 Countries assigned to the "North" community consistently in Sessions 46–63 (see Fig. 2). These countries are colored orange in Fig. 3.

Albania	Estonia	Israel	Marshall Islands	Spain
Armenia	Finland	Italy	Netherlands	Sweden
Australia	France	Japan	New Zealand	Turkey
Austria	Germany	Latvia	Norway	Ukraine
Belgium	Greece	Liechtenstein	Poland	United Kingdom
Bulgaria	Hungary	Lithuania	Portugal	United States of America
Canada	Iceland	Luxembourg	Romania	Western Samoa
Denmark	Ireland	Malta	South Korea	

4. Networks of voting agreements

We first consider the weighted, unipartite UNGA networks that we constructed by considering the level of agreement between countries. We maximize Newman–Girvan modularity, which is given by Eq. (3) with the default resolution parameter value $\gamma = 1$, for each of the UNGA sessions. To provide additional context for our discussion, we remark that modularity can be used as a measure of polarization among voting parties [21,22].

In Fig. 2, we show that beginning near the 1964 declaration of the Group of 77 (G77), the fraction of the maximum modularity value that is captured by partitioning on the basis of G77 membership tends to increase over time. In this figure, we also show the modularity value that we calculated for the two-group G77 partition (G77 members versus non-members [72]) for each session. Observe in particular a recent sharp rise in modularity in the Post-Cold-War era that was accompanied by an increase in the fraction of modularity corresponding to the G77 partition. In the right panel of the figure, we show the sizes of the communities that we found by optimizing the Newman–Girvan modularity in each session. Observe that we typically find a small number of large communities. Prior to the end of the Cold War, the dominant split appears to be along an East–West axis, which we identified by tracking specific countries (e.g., by comparing the placement of the UK and the USSR). In contrast, in the Post-Cold-War sessions, the two-community split appears to be along a "North–South" axis, illustrating the cooperation between developing countries in the dominant North–South division of the UNGA [45,47]. (In these sessions, the UK is typically assigned to the Northern bloc.) In Tables 1 and 2, respectively, we list the countries that were consistently assigned to the communities labeled "North" and "South" in Sessions 46–63 (1991–2008). In Table 1, the Marshall Islands is the only member of the G77 [73]. In Table 2, Mexico is the only non-member of the G77 (it left the organization in 1994). We depict these communities visually in Fig. 3.

Because one has to be careful with modularity's resolution limit [63], we will examine these observations more carefully in single-session case studies by incorporating resolution parameters in the appropriate null models described above. In examining the UNGA community structure over time, we consider three key eras: the early years of the Cold War (Sessions 1–25; 1946–1970), a transitional period (Sessions 26–45; 1971–1990), and the Post-Cold-War era (Sessions 46–63; 1991–2008). We consider one case study from each era – Sessions 11, 36, and 58 – and start by optimizing modularity using the null model from Eq. (3) for a large range of values of the resolution parameter γ. We start approximately from the value at which network begins to split up and end when we obtain a set of communities that consist of individual countries. We seek regions of resolution parameter values that have identical or very similar community partitions, which in turn suggests that we have detected robust mesoscopic features of the network [8,9,28,64,74]. The sizes of such regions can also potentially

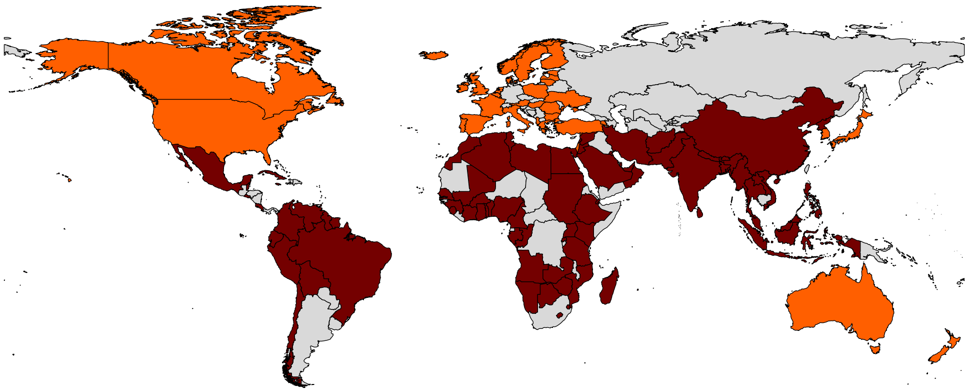

Fig. 3. (Color online) Depiction of the "North" community listed in Table 1 (orange) and the "South" community listed in Table 2 (dark red). (For interpretation of the references to color in this figure legend, the reader is referred to the online version of this article.)

Table 2
84 Countries assigned to the "South" community consistently in Sessions 46–63 (see Fig. 2). These countries are colored dark red in Fig. 3.

Afghanistan	Chile	Guinea	Maldives	Qatar	Trinidad and Tobago
Algeria	China	Guyana	Mali	Rwanda	Tunisia
Angola	Colombia	India	Mauritius	Saudi Arabia	Uganda
Bahrain	Comoros	Indonesia	Mexico	Senegal	United Arab Emirates
Bangladesh	Congo	Iran	Morocco	Sierra Leone	Venezuela
Belize	Costa Rica	Jamaica	Mozambique	Singapore	Vietnam
Benin	Côte d'Ivoire	Jordan	Myanmar	Sri Lanka	Yemen
Bhutan	Cuba	Kenya	Namibia	St. Lucia	Zambia
Bolivia	Djibouti	Kuwait	Nepal	Sudan	Zimbabwe
Botswana	Ecuador	Laos	Nigeria	Surinam	
Brazil	Egypt	Lebanon	North Korea	Swaziland	
Brunei	El Salvador	Lesotho	Oman	Syria	
Burkina Faso	Ethiopia	Libya	Pakistan	Tanzania	
Cameroon	Gabon	Madagascar	Peru	Thailand	
Cape Verde	Ghana	Malaysia	Philippines	Togo	

provide hints about the extent of such robustness. To find meaningful values of γ, we track changes between the numbers of communities obtained at "neighboring" parameter values and seek large regions (that is, plateaus) in which the network is partitioned into the same number of communities. (We define "neighboring" parameter values using a granularity $\Delta\gamma$ between the consecutive values of γ that we consider.) We also quantify changes between neighboring partitions using the Jaccard distance, although other quantities (such as variation of information) can also be used [8,24,75]. We show the Jaccard distance between neighboring values of γ for Session 11 in the top left panel of Fig. 4. When the Jaccard distance between the partitions obtained at two nearby resolution parameter values is small, then one has obtained a similar partitioning at those two values. We use such figures to indicate "robust" communities, and we seek *similar* partitions at nearby resolution parameter values. (It is important that they need not be the same.) Accordingly, the identification of a "robust" feature necessarily maintains an element of arbitrariness.

To assist in the visualization of common associations, we sorted the UNGA member countries using the set of community assignments in the network partitions that we computed. We color-coded the community assignments of the (sorted) countries at each resolution parameter value in order to highlight the sizes and similarities of communities that we obtained for different values of the resolution parameter. In the bottom left panel of Fig. 4, we illustrate the communities that we obtained for Session 11. There is a large region ($0.8 \lesssim \gamma \lesssim 1$) of two-community partitions that differ only in the placement of five countries (Finland, Cambodia, Ethiopia, Iraq, and Japan). The persistent reddish orange community in this parameter value range is the "East" group of countries, and the persistent yellow group of countries is the "West" community. Importantly, we have not sought to algorithmically identify correspondences between communities that we obtained at different resolution parameter values, so the similar coloring arises only because of the ordering of the communities after the sorting of the countries. Increasing the resolution parameter value splits the Western community into several much smaller communities (including some that consist of individual countries), leaving a small core bloc (see Table 3 and Fig. 5) of countries that are robustly placed together for values of γ up to and including the plateau observed for $\gamma \in (1.353, 1.388)$. That is, at a given value of the resolution parameter, these countries have similar colors, but the precise color of this bloc is in general different for different values of γ. Countries in the core group inside the Western bloc agree more with each other than they do with the rest of the Western bloc. Meanwhile, the Eastern community splits into two groups, which we list in Table 3 and show in the map in Fig. 5. There is a group that votes "no" on 43% of the resolutions (and abstains on 10% of them) and another that abstains on 34% of the resolutions (and votes "no" on 9% of them). The group of countries that votes "no" also tends to agree less with the West than the countries in the "abstain" group.

Table 3
Countries in the large robust groups of the Session 11 voting agreement network (highlighted in Fig. 4 using dashed lines). We show these three blocs in Fig. 5.

Western core community	Eastern community		
	"No"-voting community	Abstaining community	
United Kingdom	Poland	Yugoslavia	Morocco
Netherlands	Hungary	Libya	Sudan
Belgium	Czechoslovakia	Egypt	Syria
Luxembourg	Albania	Lebanon	Jordan
France	Bulgaria	Saudi Arabia	Yemen
Portugal	Romania	Afghanistan	India
South Africa	Russia	Myanmar	Sri Lanka
Israel	Ukraine	Indonesia	
Australia	Belarus		
New Zealand			

Table 4
Countries in the two large robust groups of the Session 36 voting agreement network (highlighted in Fig. 4 using dashed lines). We show these countries in Fig. 6.

Western community			Eastern community	
USA	Canada	UK	Cuba	East Germany
Guatemala	Paraguay	Belize	Poland	Hungary
Ireland	Netherlands	Belgium	Czechoslovakia	Albania
Luxembourg	France	Spain	Bulgaria	Russia
Portugal	West Germany	Austria	Ukraine	Belarus
Italy	Greece	Turkey	Seychelles	
Sweden	Norway	Denmark	Mongolia	
Finland	Iceland	Malawi	Vietnam	
Israel	New Zealand	Australia	Laos	
Japan			Afghanistan	

Table 5
Countries in the large robust group of the Session 58 voting agreement network (highlighted in Fig. 4 using dashed lines). We show these countries in Fig. 7.

North community		
United States of America	Canada	United Kingdom
Ireland	Netherlands	Belgium
Luxembourg	France	Monaco
Liechtenstein	Switzerland	Spain
Andorra	Portugal	German Federal Republic
Poland	Austria	Hungary
Czech Republic	Slovakia	Italy
San Marino	Malta	Albania
Macedonia	Croatia	Yugoslavia
Bosnia–Herzegovina	Slovenia	Greece
Cyprus	Bulgaria	Moldova
Romania	Estonia	Latvia
Lithuania	Georgia	Finland
Sweden	Norway	Denmark
Iceland	Turkey	Israel
South Korea	Japan	Australia
New Zealand	Marshall Islands	Palau
Federated States of Micronesia		

Although the community sizes in Session 36 and Session 58 drop off faster as the resolution parameter value increases (see, respectively, the center and right panels of Fig. 4) than is the case in Session 11, we again find a dominant two-community region for both sessions. This region starts when γ is below 0.9 and extends slightly above $\gamma \approx 1$. For Session 36, we list the countries in the Eastern-bloc and Western-bloc communities in Table 4 and show them on a map in Fig. 6. Session 36 also has a small plateau with three communities when γ is just above 1. In Session 58, the dominant two-community split divides countries into North and South groups (as we indicated previously for $\gamma = 1$), and we similarly find a small plateau in which the network is partitioned into three communities for γ just above 1. After these communities split up with a further increase of γ, we do not find any plateaus of reasonable size that correspond to network partitions with more communities, and only one group of countries (the North group listed in Table 5 and depicted in Fig. 7) appears to be robust throughout this range of γ values. As indicated by the dashed lines in Fig. 4, we have not required all countries in such a "robust" group

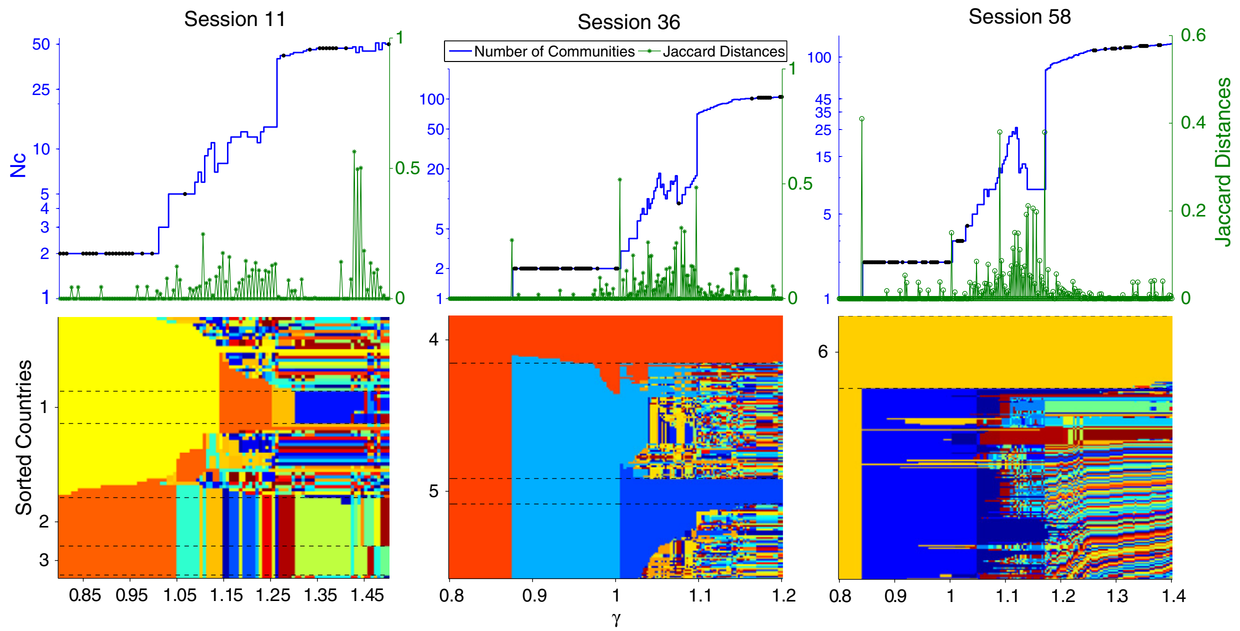

Fig. 4. (Color online) Results of community detection in (left) Session 11, (center) Session 36, and (right) Session 58 of the UNGA by optimizing the modularity in (3) for the network of voting similarities. (Top) Number of communities (N_c; blue) that we obtained at each value of the resolution parameter γ and the Jaccard distance (green) between partitions obtained at neighboring values of γ (which differ by $\Delta\gamma \approx 0.007$, 0.002, and 0.003, respectively, in Sessions 11, 36, and 58). (Bottom) Community assignments at each value of γ. We sort countries vertically according to their community assignments for the range of γ values in order to keep countries that are commonly grouped together close to each other in the sorting. We use color to visualize each community at a given resolution parameter value without explicit identification of correspondence between communities at different resolution parameter values. (Hence, the color that corresponds to a commonly-grouped community can be different for different values of the resolution parameter.) In Table 3, we indicate the three sets of countries in Session 11 that we identify as grouped together robustly for the plotted range of resolution parameter values: (1) the Western core of countries that are commonly grouped together and an Eastern community containing groups of (2) abstaining countries and (3) "No"-voting countries. In Table 4, we similarly indicate the two groups of countries that we identify as arising robustly in Session 36: (4) a Western group and (5) an Eastern group. In Table 5, we identify a robust group of countries in Session 58 as (6) a "North" community. (Note that our visualization repeats some of the community colors for countries that do not appear near each other in these plots when the number of communities is large; this has no additional significance.)

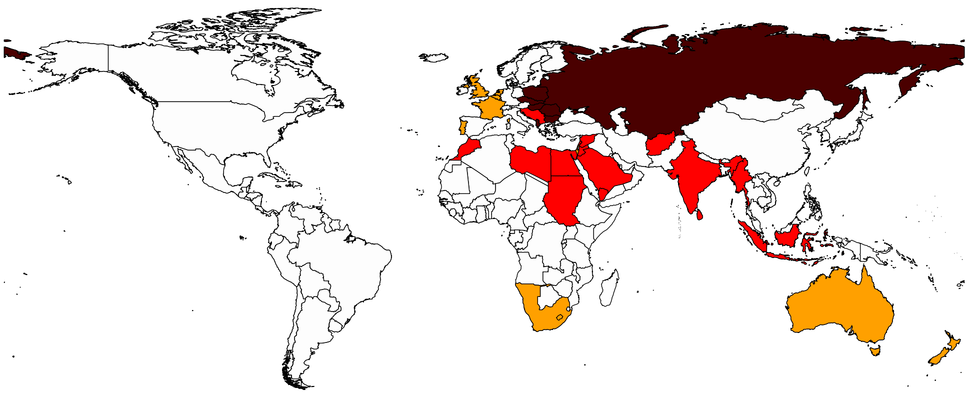

Fig. 5. (Color online) Depiction of the community cores for the Session 11 voting agreement network. We list the countries in these cores in Table 3: Western-bloc core (yellowish orange), Eastern "abstain" group (bright red), and Eastern "no" subgroup (dark red). (The 1958 map data available to us for plotting was incomplete, so we made all of our Session 11 maps with 1958 data overlaid on uncolored 2000 map data. This way, the holes in the 1958 map are filled by current data, and the coloring of countries that we highlight are accurate for the time period.) (For interpretation of the references to color in this figure legend, the reader is referred to the online version of this article.)

to always appear together. Rather, we have demarcated these groups within the plots according to their preponderance in the partitions that we considered. Other, less arbitrary, means of identifying robust groups can be used (e.g., one might require a minimum number of common pairwise assignments), and this would be necessary for investigations of larger systems.

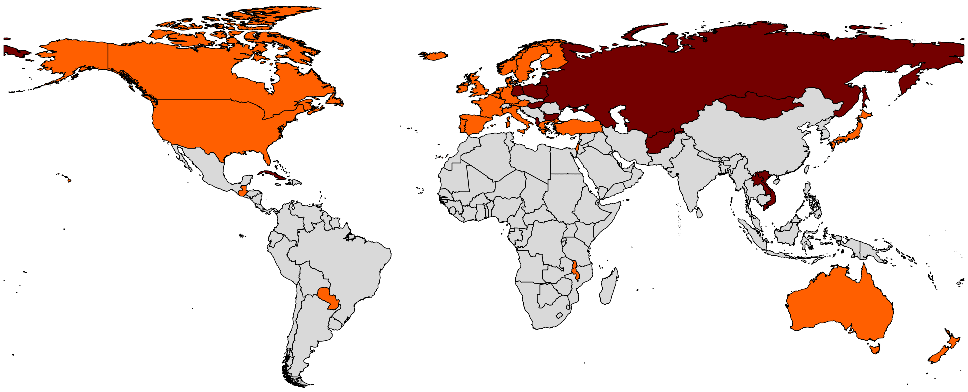

Fig. 6. (Color online) Depiction of the two large robust groups that we identified in the Session 36 voting agreement network. We list the countries in these groups in Table 4: West (orange) and East (dark red). (For interpretation of the references to color in this figure legend, the reader is referred to the online version of this article.)

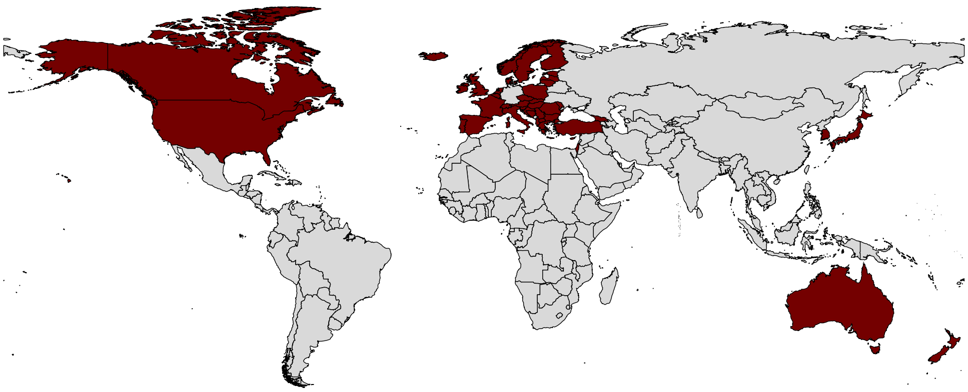

Fig. 7. (Color online) The robust "North" group that we identified in the Session 58 voting agreement network. We list the countries in this group in Table 5.

5. Networks of voting agreements and disagreements

In this section, we study the signed unipartite networks that we obtain by treating the positive and negative edges separately. As indicated in Section 3, this yields a null model with two terms and a resolution parameter (γ and λ) for each of them. Using the network of agreements and disagreements described in Section 2, we sweep over different values of the two resolution parameters and plot surfaces for the numbers of communities in Fig. 8. In these plots, we have color-coded each surface by the mean Jaccard distances between each partition and its nearest neighbors in resolution parameter space. That is, given the square grid of sampled resolution parameter values that we explore, we compare each partition with its four nearest neighbors.

In this two-dimensional resolution parameter space, one can no longer easily visualize all of the community assignments at each resolution parameter value. Because we seek robust community assignments, we avoid parameter values near which the number of communities (indicated by the height in the left panels of Fig. 8) changes rapidly. In order to ensure similarities in nearby partitions (as it is insufficient to only consider the same numbers of communities), we calculate the Jaccard distances between the partitions that we obtained at nearest-neighbor points on a square grid in the (γ, λ) plane. We consider $\gamma, \lambda \in [0, 2]$ and discretize both parameters using 101 uniformly-spaced points. We have color-coded the left panels of Fig. 8 at each grid point according to the mean Jaccard distance between that partition and its four nearest neighbors. We then select points on this grid by hand that yield partitions that persist over a range of resolution parameter values. For each of our three case studies (Sessions 11, 36, and 58), we show the number of communities and mean Jaccard distance at the selected points in resolution parameter space. In Fig. 8, we have also tabulated the resolution parameter values and the partitions that we found at the selected points in parameter space. In agreement with the results in Section 4, we recover the dominant two-way split in the UNGA that spans a large portion of the parameter space. In the far right of the figure, we identify groups of countries that are placed together at all of the selected resolution parameter values, thereby finding some smaller robust groups. Observe in Sessions 11 and 58 (and to a lesser extent in Session 36) that some communities of moderate and even large size persist robustly even when each of the countries not in those communities is

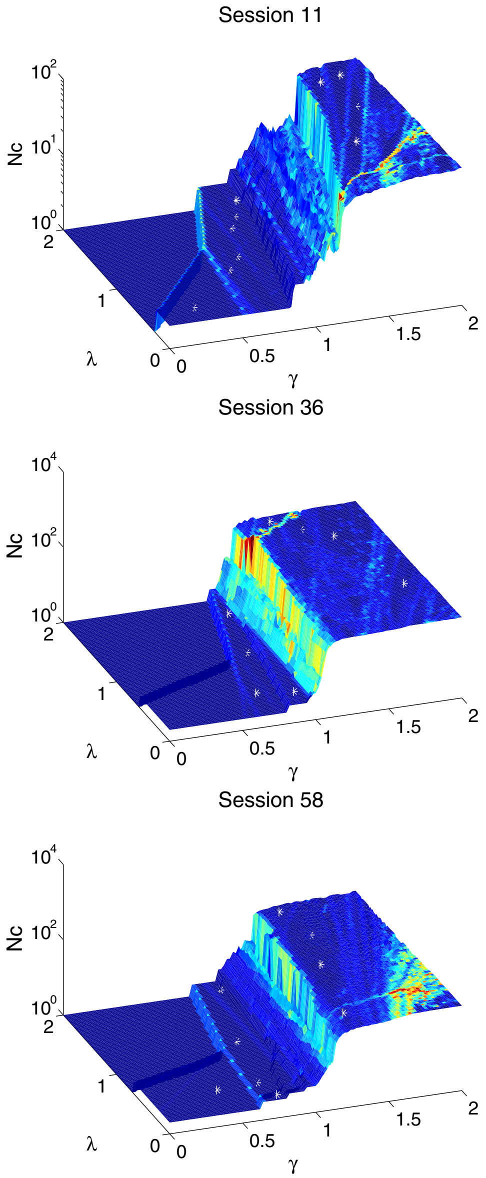

Index	γ	λ
1	.24	.22
2	.66	.70
3	.78	.88
4	.90	1.32
5	.98	1.48
6	1.08	1.72
7	1.68	1.78
8	1.82	1.80
9	1.74	1.28
10	1.56	.78

Index	γ	λ
1	.72	.36
2	.92	.20
3	.88	.98
4	.98	1.60
5	1.38	1.92
6	1.52	1.72
7	1.68	1.54
8	1.84	.66

Index	γ	λ
1	.46	.38
2	.76	.08
3	.74	.40
4	.84	1.06
5	1.02	1.86
6	1.44	1.90
7	1.50	1.48
8	1.40	1.02
9	1.28	.26

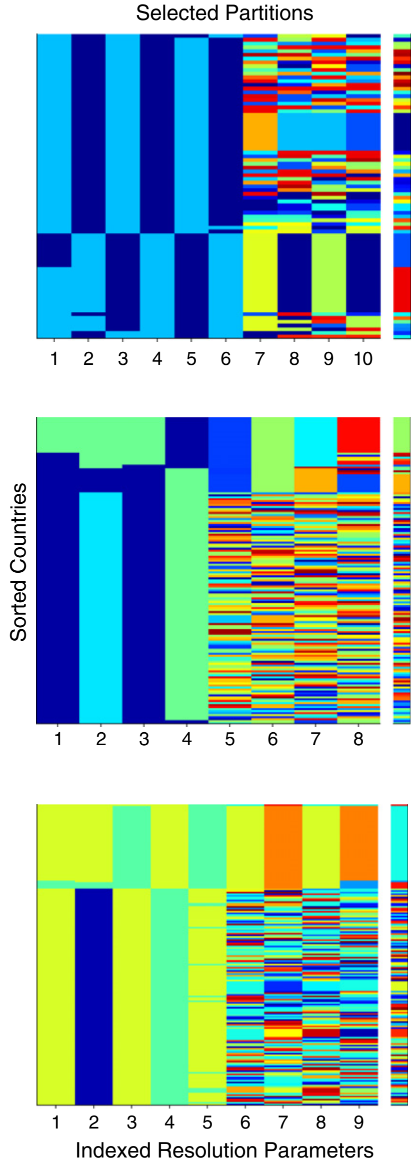

Fig. 8. (Color online) Exploration of the space of resolution parameters for the signed unipartite network of countries in (top) Session 11, (middle) Session 36, and (bottom) Session 58 of the UNGA. (Left) Number of communities identified at each pair of resolution parameter values. We have color-coded these plots according to the mean Jaccard distance between a partition and its four nearest neighbors in resolution parameter space. We consider $\gamma, \lambda \in [0, 2]$ and discretize both parameters using 101 uniformly-spaced points. (Center) Resolution parameter values (selected by hand) in different robust regions of the resolution parameter space. (Right) Color-coded visualization of the communities obtained at each indexed point in resolution parameter space. The column at the far right color-codes the blocks of countries that are grouped together robustly for all of the indexed partitions. (As in prior figures, there is no correspondence between the colors that we used for different resolution parameter values.)

assigned to its own individual community or to some tiny community. We identify the countries in these robust communities for Session 11, 36, and 58 in Tables 6–8, and we show them on maps in Figs. 9–11.

6. Bipartite voting networks with positive and negative edges

In this section, we use the signed bipartite modularity from Section 3 to study networks of yes and no votes, which we represent using positive and negative edges between UNGA countries and the resolutions on which they voted. (We do not include abstentions in this representation.) As before, we seek robust communities by exploring the two-dimensional space of resolution parameter values, examining the numbers of communities at neighboring points in the space, and calculating the mean Jaccard distances between the partitions obtained at nearest-neighbor resolution parameter values on a uniform

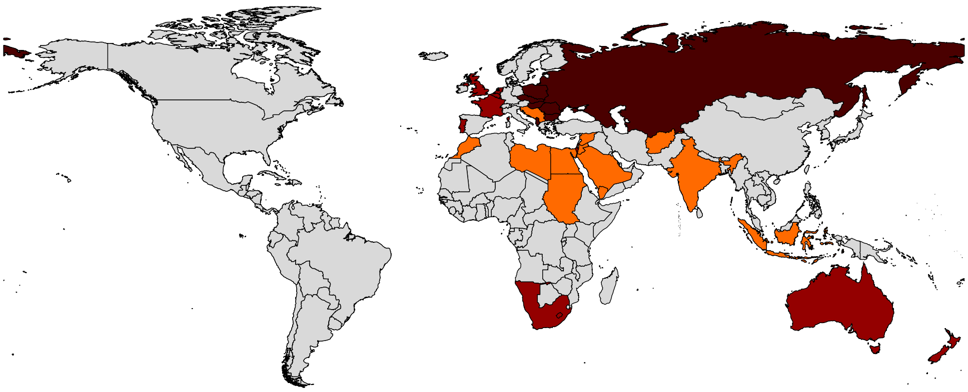

Fig. 9. (Color online) Depiction of the three robust groups of countries in Table 6 for the Session 11 network of voting agreements and disagreements. We show group 1 in yellowish orange, group 2 in red, and group 3 in dark red. (For interpretation of the references to color in this figure legend, the reader is referred to the online version of this article.)

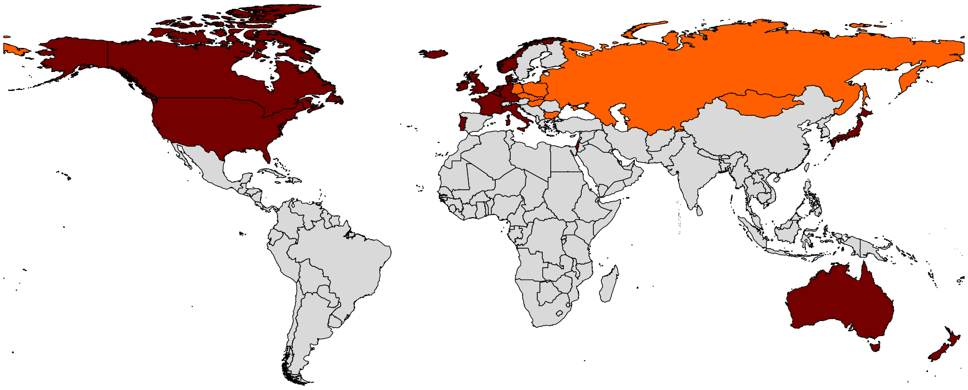

Fig. 10. (Color online) Depiction of the two robust groups of countries in Table 7 for the Session 36 network of voting agreements and disagreements. We show group 1 in dark red and group 2 in orange. (For interpretation of the references to color in this figure legend, the reader is referred to the online version of this article.)

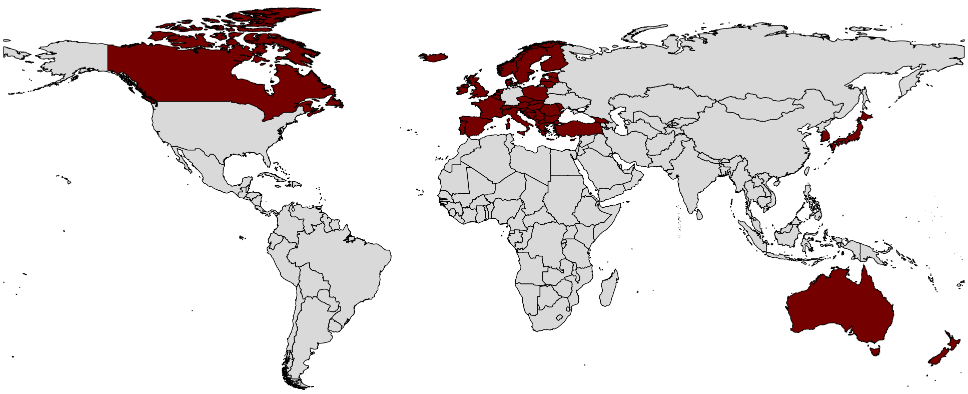

Fig. 11. (Color online) Depiction of the robust group of countries in Table 8 for the Session 58 network of voting agreements and disagreements.

grid with $\gamma, \lambda \in [0, 2]$. We calculate the Jaccard distances that we used for these partitions with respect to the full bipartite networks (rather than restricting to the partitions of countries).

We show the results of our numerical exploration of the signed bipartite networks in Fig. 12. A major difference between our results for these networks and those reported in the previous sections is that community detection on the bipartite networks also includes UNGA resolutions in the groups with the countries that predominantly supported such sets of resolutions. We find that the UNGA sessions in each of our three case studies include numerous resolution parameter values (indicated in Fig. 12) in which there are large, robust communities (in agreement with our observations using the other network formulations). Session 11 contains resolution parameter values in which one of these two robust communities is

Table 6
Countries in the robust groups of the Session 11 network of voting agreements and disagreements (see Figs. 8 and 9).

1	2	3
Yugoslavia	United Kingdom	Poland
Morocco	Netherlands	Hungary
Libya	Belgium	Czechoslovakia
Sudan	Luxembourg	Albania
Egypt	France	Bulgaria
Syria	Portugal	Romania
Jordan	South Africa	Russia
Saudi Arabia	Israel	Ukraine
Yemen	Australia	Belarus
Afghanistan	New Zealand	
India		
Indonesia		

Table 7
Countries in the robust groups of the Session 36 network of voting agreements and disagreements (see Figs. 8 and 10).

1		2
United States of America	German Federal Republic	German Democratic Republic
Canada	Italy	Poland
United Kingdom	Norway	Hungary
Ireland	Denmark	Czechoslovakia
Netherlands	Iceland	Bulgaria
Belgium	Israel	Russia
Luxembourg	Japan	Ukraine
France	Australia	Belarus
Portugal	New Zealand	Mongolia

Table 8
Countries appearing in the single robust group of the Session 58 network of voting agreements and disagreements (see Figs. 8 and 11).

Canada	Spain	San Marino	Bulgaria	Denmark
United Kingdom	Andorra	Malta	Moldova	Iceland
Ireland	Portugal	Albania	Romania	Turkey
Netherlands	Germany	Macedonia	Estonia	South Korea
Belgium	Poland	Croatia	Latvia	Japan
Luxembourg	Austria	Yugoslavia	Lithuania	Australia
France	Hungary	Bosnia–Herzegovina	Georgia	New Zealand
Monaco	Czech Republic	Slovenia	Finland	
Liechtenstein	Slovakia	Greece	Sweden	
Switzerland	Italy	Cyprus	Norway	

much larger than the other one. Sessions 36 and 58 both contain regions in which there is one dominant community that contains almost every country. In contrast to the other network representations, we note that there do not appear to be any robust plateau regions for $\gamma > 1$. This feature is illustrated in Fig. 12 and should be compared to the results we showed in Figs. 4 and 8. Each of the robust partitions indicated in Fig. 12 consists of two large groups, and only a few countries are assigned to other groups. Although the network partitions in Fig. 12 differ from one another for different resolution parameter values, many of the community assignments in these partitions nevertheless remain the same for many points in resolution parameter space. In the far right of the figure, we identify groups of countries and resolutions that are placed together at all of the indexed resolution parameter values in Fig. 12. We list the countries in the larger such groups for Sessions 11, 36, and 58 in Tables 9, 10 and 11, respectively. We show these same groups of countries on maps in Figs. 13–15, respectively.

7. Conclusions and discussion

We have studied community structure in networks formed by voting on resolutions in individual sessions of the United Nations General Assembly. The UNGA voting record provides a fascinating example of a very general problem: How can one use network methods such as community detection to examine data such as voting records? Accordingly, our focus is not on attempting a sociological or political study of the UNGA but rather on using it as an interesting and potentially valuable example for which we consider different network representations that are each reasonable and subsequently compare our results from each of them. To do this, we constructed networks from the UNGA voting records of sixty-three separate sessions

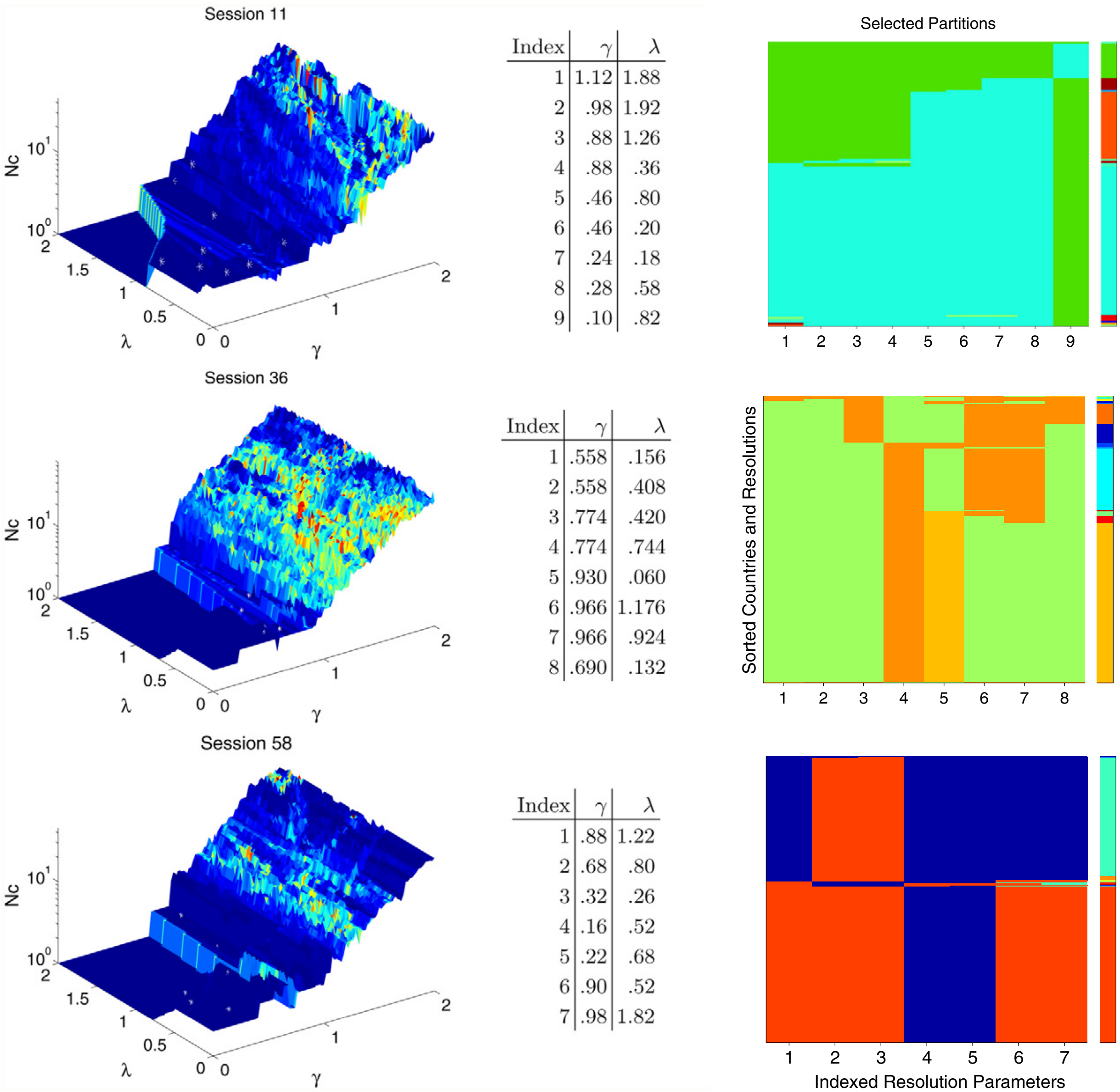

Index	γ	λ
1	1.12	1.88
2	.98	1.92
3	.88	1.26
4	.88	.36
5	.46	.80
6	.46	.20
7	.24	.18
8	.28	.58
9	.10	.82

Index	γ	λ
1	.558	.156
2	.558	.408
3	.774	.420
4	.774	.744
5	.930	.060
6	.966	1.176
7	.966	.924
8	.690	.132

Index	γ	λ
1	.88	1.22
2	.68	.80
3	.32	.26
4	.16	.52
5	.22	.68
6	.90	.52
7	.98	1.82

Fig. 12. (Color online) Exploration of the resolution parameter space for the signed bipartite network of countries and resolutions in (top) Session 11, (middle) Session 36, and (bottom) Session 58 of the UNGA. (Left) Number of communities that we identified for each value of the pair of resolution parameters. We have color-coded these plots according to the mean Jaccard distance (which we computed for the full bipartite network) between the partition and its four nearest neighbors in resolution parameter space. We again consider $\gamma, \lambda \in [0, 2]$ and discretize both parameters using 101 uniformly-spaced points. (Center) Resolution parameter values (selected by hand) for different robust regions in the resolution parameter space. (Right) Color-coded visualization of the communities that we obtained at each indexed point in resolution parameter space. The far right column color-codes the blocks of countries and resolutions that are grouped together robustly for all of the indexed partitions. (As in prior figures, there is no correspondence between the colors that we used for different resolution parameter values.)

between 1946 and 2008 in three different ways: (1) by considering voting similarities as weighted unipartite networks by counting agreements, (2) by considering voting similarities as weighted unipartite networks in a manner that separately counts agreements and disagreements, and (3) as signed bipartite networks in which countries are connected to resolutions. For each formulation, we detected communities by optimizing network modularity using an appropriate null model. In optimizing a quality function such as modularity, the consideration of multiple resolution parameters enables us to examine different "background" levels of agreement between nations.

In Fig. 16, we compare the community detection results that we obtained by partitioning the countries using the three different network representations on each of our "case-study" sessions of the UNGA (Sessions 11, 36, and 58). We consider modularity-optimizing partitions of the network of agreements at two different values of the resolution parameter ($\gamma_1 = 1$

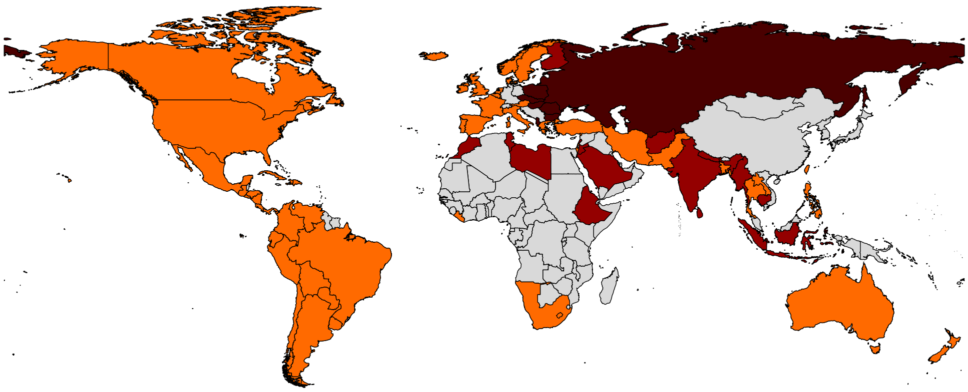

Fig. 13. (Color online) Depiction of the three groups in the Session 11 signed bipartite voting network. We list these countries in Table 9 and show group 1 in dark red, group 2 in red, and group 3 in orange. (For interpretation of the references to color in this figure legend, the reader is referred to the online version of this article.)

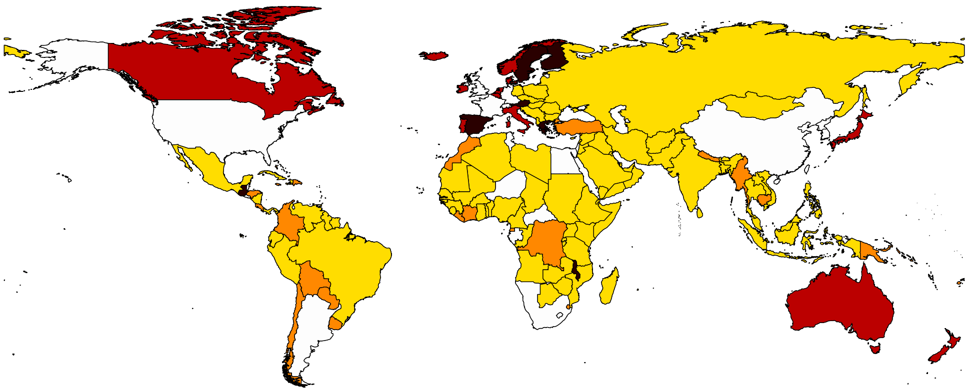

Fig. 14. (Color online) Depiction of the four groups in the Session 36 signed bipartite voting network. We list these countries in Table 10 and show group 1 in dark red, group 2 in red, group 3 in yellowish orange, and group 4 in yellow. (For interpretation of the references to color in this figure legend, the reader is referred to the online version of this article.)

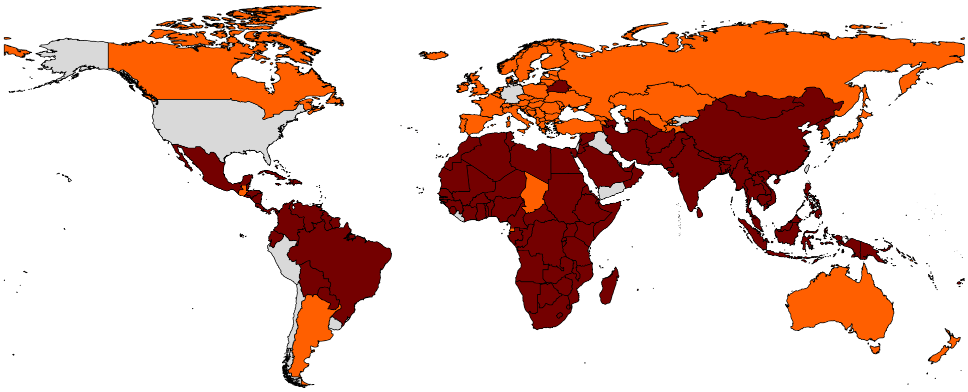

Fig. 15. (Color online) Depiction of the two groups of the Session 58 signed bipartite voting network. We list these countries in Table 11 and show group 1 in orange and group 2 in dark red. (For interpretation of the references to color in this figure legend, the reader is referred to the online version of this article.)

and $\gamma_2 > 1$; see the figure caption for the values of γ_2 for each session) and illustrate the robust groups that we identified for the indexed points in the resolution parameter spaces of the signed unipartite network representation and the signed bipartite network representation. (For the latter, we only show the groups of countries, but there are resolutions that go with them.) For each network representation, we find a dominant voting pattern that includes two large communities corresponding to majority and minority groups. We observed this feature for each of the three UNGA sessions in our case studies. This split appears most clearly for the partitions that we obtained using modularity optimization of the agreement

Table 9
Countries in the three largest robust groups of the Session 11 bipartite network (see Figs. 12 and 13). We grouped resolutions (not listed) with these countries by detecting communities in the signed bipartite network of countries and resolutions.

1	2	3		
Poland	Finland	United States of America	Bolivia	Sweden
Hungary	Ethiopia	Canada	Paraguay	Norway
Czechoslovakia	Morocco	Cuba	Chile	Denmark
Albania	Tunisia	Haiti	Argentina	Iceland
Bulgaria	Libya	Dominican Republic	Uruguay	Liberia
Romania	Lebanon	Mexico	United Kingdom	South Africa
Russia	Jordan	Guatemala	Ireland	Iran
Ukraine	Saudi Arabia	Honduras	Netherlands	Turkey
Belarus	Afghanistan	El Salvador	Belgium	Israel
	India	Nicaragua	Luxembourg	Taiwan
	Myanmar	Costa Rica	France	Pakistan
	Sri Lanka	Panama	Spain	Thailand
	Nepal	Colombia	Portugal	Laos
	Cambodia	Venezuela	Austria	Philippines
	Indonesia	Ecuador	Italy	Australia
		Peru	Greece	New Zealand
		Brazil		

Table 10
Countries in the four largest robust groups of the Session 36 bipartite network (see Figs. 12 and 14; resolutions not listed).

1	2	3	4		
Guatemala	Canada	Bahamas	Cuba	Guinea-Bissau	Algeria
Spain	Ireland	Dominican Republic	Haiti	Gambia	Libya
Austria	Netherlands	Jamaica	Trinidad and Tobago	Mali	Sudan
Greece	Belgium	Belize	Barbados	Senegal	Iran
Finland	Luxembourg	Honduras	Grenada	Benin	Iraq
Sweden	Portugal	Costa Rica	St. Lucia	Mauritania	Syria
Malawi	Italy	Colombia	St. Vincent and the Grenadines	Guinea	Lebanon
	Norway	Bolivia	Antiqua and Barbuda	Burkina Faso	Jordan
	Denmark	Paraguay	Mexico	Sierra Leone	Saudi Arabia
	Iceland	Chile	Nicaragua	Ghana	Arab Republic of Yemen
	Japan	Uruguay	Panama	Togo	Peoples Republic of Yemen
	Australia	Equatorial Guinea	Venezuela	Cameroon	Kuwait
	New Zealand	Côte d'Ivoire	Guyana	Nigeria	Bahrain
		Liberia	Surinam	Chad	Qatar
		Congo	Ecuador	Congo	United Arab Emirates
		Swaziland	Peru	Uganda	Oman
		Morocco	Brazil	Kenya	Afghanistan
		Turkey	German Democratic Republic	Tanzania	Mongolia
		Myanmar	Poland	Burundi	India
		Nepal	Hungary	Rwanda	Bhutan
		Cambodia	Czechoslovakia	Somalia	Pakistan
		Singapore	Malta	Djibouti	Bangladesh
		Papua New Guinea	Albania	Ethiopia	Sri Lanka
		Solomon Islands	Yugoslavia	Angola	Maldives
		Fiji	Cyprus	Mozambique	Thailand
		Western Samoa	Bulgaria	Zambia	Laos
			Romania	Zimbabwe	Vietnam
			Russia	Botswana	Malaysia
			Ukraine	Madagascar	Philippines
			Belarus	Comoros	Indonesia
			Cape Verde	Mauritius	
			Sao Tome & Principe	Seychelles	

networks at the standard resolution parameter value $\gamma_1 = 1$ (first column) and those that we obtained using modularity optimization of the bipartite networks (fourth column). Additionally, one can see (by comparing the first column to the second column) small and medium-size cores of groups in the networks of agreements that persist for $\gamma_2 > 1$. For all three case-study sessions, we find such core groups in the second column that arise from each of the large communities in the first column. In each of the sessions, large portions of these core communities remain intact when considering networks of both agreements and disagreements (third column). These observations appear to be consistent with the expected East–West split of the Cold War and the North–South division of recent sessions that has been described by Lloyd using qualitative methods [45].

Table 11
Countries in the two large robust groups of the Session 58 bipartite network (see Figs. 12 and 15; resolutions not listed).

1		2			
Canada	Greece	Bahamas	Senegal	Lesotho	Myanmar
St. Vincent & the Grenadines	Cyprus	Cuba	Benin	Botswana	Sri Lanka
St. Kitts-Nevis	Bulgaria	Haiti	Mauritania	Swaziland	Maldives
Guatemala	Moldova	Dominican Republic	Niger	Madagascar	Nepal
Argentina	Romania	Jamaica	Côte d'Ivoire	Comoros	Thailand
United Kingdom	Russia	Trinidad and Tobago	Guinea	Mauritius	Cambodia
Ireland	Estonia	Barbados	Burkina Faso	Morocco	Laos
Netherlands	Latvia	Dominica	Sierra Leone	Algeria	Vietnam
Belgium	Lithuania	Grenada	Ghana	Tunisia	Malaysia
Luxembourg	Ukraine	St. Lucia	Togo	Libya	Singapore
France	Armenia	Antiqua and Barbuda	Cameroon	Sudan	Brunei
Monaco	Georgia	Mexico	Nigeria	Iran	Philippines
Liechtenstein	Finland	Belize	Gabon	Egypt	Indonesia
Switzerland	Sweden	Honduras	Central African Rep.	Syria	Papua New Guinea
Spain	Norway	El Salvador	Congo	Lebanon	Vanuatu
Andorra	Denmark	Nicaragua	Dem. Rep. of Congo	Jordan	Fiji
Portugal	Iceland	Costa Rica	Uganda	Saudi Arabia	Nauru
German Fed. Rep.	Sao Tome & Principe	Panama	Kenya	Arab Rep. of Yemen	Tonga
Poland	Equatorial Guinea	Colombia	Tanzania	Kuwait	
Austria	Chad	Venezuela	Burundi	Bahrain	
Hungary	Turkey	Guyana	Rwanda	Qatar	
Czech Republic	Tajikistan	Surinam	Somalia	United Arab Emirates	
Slovakia	Uzbekistan	Ecuador	Djibouti	Oman	
Italy	Kazakhstan	Brazil	Ethiopia	Afghanistan	
San Marino	South Korea	Bolivia	Eritrea	Turkmenistan	
Malta	Japan	Paraguay	Angola	China	
Albania	Australia	Belarus	Mozambique	Mongolia	
Macedonia	New Zealand	Azerbaijan	Zambia	North Korea	
Croatia	Solomon Islands	Cape Verde	Zimbabwe	India	
Yugoslavia	Kiribati	Guinea-Bissau	Malawi	Bhutan	
Bosnia–Herzegovina	Tuvalu	Gambia	South Africa	Pakistan	
Slovenia	Western Samoa	Mali	Namibia	Bangladesh	

In the present paper, we chose to examine the robustness of network partitions with respect to perturbations of resolution parameters. Because we had two such parameters, this entailed extensive numerical calculation, but it does not exhaust the types of partition robustness that one might want to consider. For example, one could perturb the networks themselves by randomizing links and then study the stability of partitions with respect to such perturbations [76]. Similarly, one could use multiple runs of a single community detection method (e.g., by randomizing the order of nodes in the Louvain method [60]), as this would provide an ensemble of slightly different results that could be used to measure partition robustness [77]. Alternatively, one could use multiple such runs or use multiple quality-optimization methods to quantify statistics of the nearly-optimal landscape of partitions (as opposed to selecting the highest-quality partition obtained using multiple computational heuristics, which is what we have done).

In principle, the bipartite network representation would seem to be better than our other representations for investigations of voting, as it contains the complete record of votes cast on resolutions. However, we have observed in our comparison of the communities that we identified that the predominant groupings of countries also appear prominently when employing the other network representations. Moreover, in our examples, community detection on the bipartite voting network tends to only return large groups – and few partitions seem to be robust at higher resolution parameter values – whereas the other network representations uncovered a more diverse set of robust groups, including small groups of countries, which complements the information contained in the large-group partitions. These differences illustrate the importance of considering multiple network representations in the investigation of voting networks and, more generally, that it is crucial to be cognizant of multiple possible network representations when applying network methods.

In this paper, we considered individual UNGA sessions as static networks and investigated how their community structure changes over time. This investigation serves as a crucial preparatory step for employing our new method of multislice modularity optimization [30], which would allow one to examine community structure in this time-dependent data without examining different sessions as separate, static objects. The present investigation – whose goal was the comparison of different ways to turn voting data into network representations – is a necessary precursor for the meaningful application of techniques such as multislice community detection, as it allows one to carefully probe the data representation and resolution parameter values to be used in such calculations in the future.

Acknowledgments

We thank Eric Voeten and Adis Merdzanovic for the United Nations voting data [78] and James Fowler, Yonatan Lupu, Mark Newman, and Vincent Traag for useful discussions. We also thank the anonymous referees for their helpful comments on the paper. KTM was funded in part by a Summer Undergraduate Research Fellowship from the UNC Office of

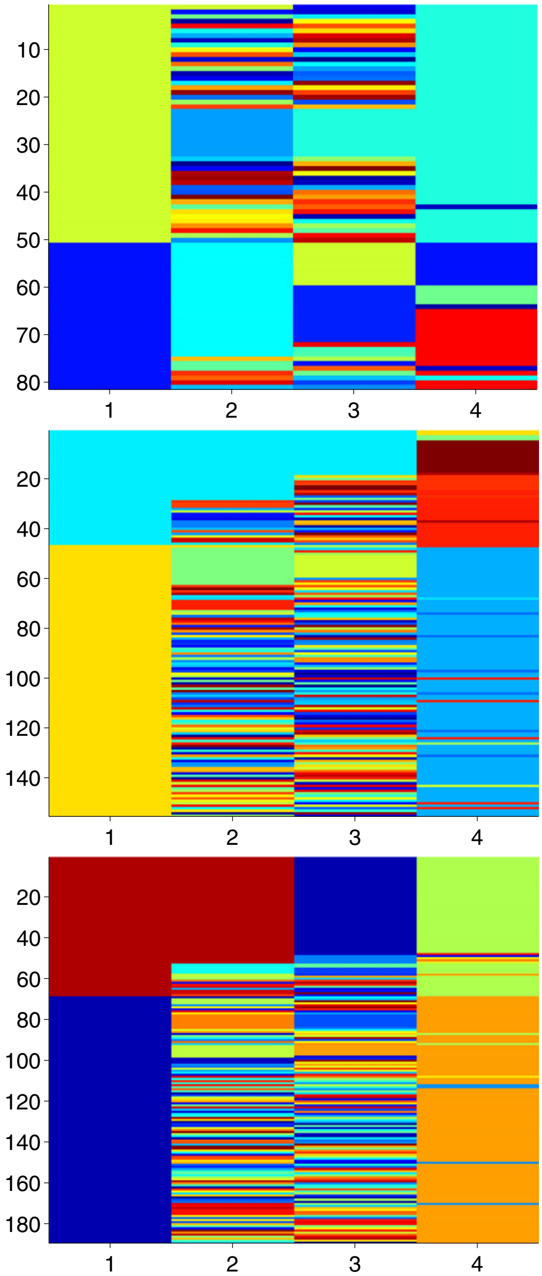

Fig. 16. (Color online) Comparison of the robust groups that we obtained using community detection for each network representation of each of our three case studies of UNGA sessions: (top) Session 11, (middle) Session 36, and (bottom) Session 58. For each session, we use a color-coding to visualize the robust groups. In particular, we compare (1) the partition that we obtained by modularity optimization at the default resolution parameter value ($\gamma = 1$) in the network of voting similarities; (2) the partition that we obtained by modularity optimization of the same network at resolution parameter values $\gamma \approx 1.360$ (Session 11), $\gamma \approx 1.180$ (Session 36), and $\gamma \approx 1.259$ (Session 58), where we note that each of these values is near the respective right edges of the ranges plotted in Fig. 4; (3) the robust groups that we identified at the indexed points in resolution parameter space in the signed unipartite network of voting agreements and disagreements (Fig. 8); and (4) the robust groups of countries that we identified at the indexed points in resolution parameter space in the signed bipartite network of countries and votes (see Fig. 12).

Undergraduate Research. PJM & KTM were also funded by the NSF (DMS-0645369). MAP acknowledges a research award (#220020177) from the James S. McDonnell Foundation. The map visualizations in this article were generated using the CShapes package in R [79].

References

[1] S. Wasserman, K. Faust, Social Network Analysis: Methods and Applications, Cambridge University Press, Cambridge, UK, 1994.
[2] S.H. Strogatz, Nature 410 (2001) 268.

[3] M.E.J. Newman, SIAM Review 45 (2003) 167.
[4] M.E.J. Newman, Networks: An Introduction, Oxford University Press, Oxford, UK, 2010.
[5] R. Albert, A.-L. Barabási, Reviews of Modern Physics 74 (2002) 47.
[6] S.N. Dorogovtsev, A.V. Goltsev, J.F.F. Mendes, Reviews of Modern Physics 80 (2008) 1275.
[7] G. Caldarelli, Scale-Free Networks: Complex Webs in Nature and Technology, Oxford University Press, Oxford, UK, 2007.
[8] S. Fortunato, Physics Reports 486 (2010) 75.
[9] M.A. Porter, J.-P. Onnela, P.J. Mucha, Notices of the American Mathematical Society 56 (2009) 1082.
[10] S.E. Schaeffer, Computer Science Review 1 (2007) 27.
[11] J. Moody, D.R. White, American Sociological Review 68 (2003) 103.
[12] R. Guimerà, L.A.N. Amaral, Nature 433 (2005) 895.
[13] A.C.F. Lewis, N.S. Jones, M.A. Porter, C.M. Deane, BMC Systems Biology 4 (2010) 100.
[14] A. Lancichinetti, S. Fortunato, Physical Review E 80 (2010) 056117.
[15] L. Danon, A. Diaz-Guilera, J. Duch, A. Arenas, Journal of Statistical Mechanics (2005) P09008.
[16] M. Girvan, M.E.J. Newman, Proceedings of the National Academy of Sciences 99 (2002) 7821.
[17] T. Callaghan, P.J. Mucha, M.A. Porter, American Mathematical Monthly 114 (2007) 761.
[18] M.A. Porter, P.J. Mucha, M.E.J. Newman, C.M. Warmbrand, Proceedings of the National Academy of Sciences 102 (2005) 7057.
[19] M.A. Porter, P.J. Mucha, M.E.J. Newman, A.J. Friend, Physica A 386 (2007) 414.
[20] M.A. Porter, A.J. Friend, P.J. Mucha, M.E.J. Newman, Chaos 16 (2006) 041106.
[21] Y. Zhang, A.J. Friend, A.L. Traud, M.A. Porter, J.H. Fowler, P.J. Mucha, Physica A 387 (2008) 1705.
[22] A.S. Waugh, L. Pei, J.H. Fowler, P.J. Mucha, M.A. Porter, 2011. arXiv:0907.3509.
[23] M.C. González, H.J. Herrmann, J. Kertész, T. Vicsek, Physica A 379 (2007) 307.
[24] A.L. Traud, E.D. Kelsic, P.J. Mucha, M.A. Porter, SIAM Review 53 (2011) 526.
[25] A.L. Traud, P.J. Mucha, M.A. Porter, 2011. arXiv:1102.2166.
[26] J.-P. Onnela, J. Saramäki, J. Hyvönen, G. Szabó, D. Lazer, K. Kaski, J. Kertész, A.-L. Barabási, Proceedings of the National Academy of Sciences 104 (2007) 7332.
[27] G. Palla, A.-L. Barabási, T. Vicsek, Nature 446 (2007) 664.
[28] D.J. Fenn, M.A. Porter, M. McDonald, S. Williams, N.F. Johnson, N.S. Jones, Chaos 19 (2009) 033119.
[29] D.J. Fenn, M.A. Porter, P.J. Mucha, M. McDonald, S. Williams, N.F. Johnson, N.S. Jones, 2010. arXiv:0905.4912.
[30] P.J. Mucha, T. Richardson, K. Macon, M.A. Porter, J.-P. Onnela, Science 328 (2010) 876.
[31] S. Gómez, P. Jensen, A. Arenas, Physical Review E 80 (2009) 016114.
[32] V.A. Traag, J. Bruggeman, Physical Review E 80 (2009) 036115.
[33] A. Lijphart, American Political Science Review 57 (1963) 902.
[34] K.T. Poole, H. Rosenthal, Congress: A Political-Economic History of Roll Call Voting, Oxford University Press, Oxford, UK, 1997.
[35] G. Gan, C. Ma, J. Wu, Data Clustering: Theory, Algorithms, and Applications, Society for Industrial and Applied Mathematics, Philadelphia, PA, 2007.
[36] E.M. Hafner-Burton, M. Kahler, A.H. Montgomery, International Organizations 63 (2009) 559.
[37] Z. Maoz, Journal of Peace Research 43 (2006) 391.
[38] Z. Maoz, L.G. Terris, R.D. Kuperman, I. Talmud, Journal of Politics 69 (2007) 100.
[39] Z. Maoz, The Evolution, Structure, and Impact of International Networks, 1816–2001, Cambridge University Press, Cambridge, UK, 2011.
[40] J. Pevehouse, T. Nordstrom, K. Warnke, Conflict Management and Peace Science 21 (2004) 101.
[41] P. Diehl, 2009. Available at: http://www.correlatesofwar.org/.
[42] S.J. Cranmer, R.M. Siverson, Journal of Politics 70 (2008) 794.
[43] E. Voeten, International Organizations (2000) 185.
[44] H. Riss, 2010. http://voteworld.berkeley.edu/.
[45] P. Lloyd, Mapping the world order: A reassessment of Huntington's Clash of Civilizations thesis, 2008 (unpublished).
[46] United Nations, 2009. Available at: http://www.un.org/ga/.
[47] B.M. Russet, American Political Science Review 60 (1966) 327.
[48] J.H. Fowler, Social Networks 28 (2006) 456.
[49] J.H. Fowler, Political Analysis 14 (2006) 454.
[50] E. Gartzke, 2009. Available at: http://dss.ucsd.edu/~egartzke.
[51] S. Signorino, J. Ritter, International Studies Quarterly 43 (1999) 115.
[52] K. Sweeney, O.M.G. Keshk, Conflict Management and Peace Science 22 (2009) 165.
[53] J. Cohen, Educational and Psychological Measurement 20 (1960) 37.
[54] T. Heimo, J.S. Kumpula, K. Kaski, J. Saramäki, Journal of Statistical Physics (2008) P08007.
[55] M.E.J. Newman, M. Girvan, in: R. Pastor-Satorras, J. Rubi, A. Diaz-Guilera (Eds.), Statistical Mechanics of Complex Networks, Springer-Verlag, Berlin, Germany, 2003.
[56] M.E.J. Newman, M. Girvan, Physical Review E 69 (2004) 026113.
[57] M.E.J. Newman, Physical Review E 74 (2006) 036104.
[58] M.E.J. Newman, Proceedings of the National Academy of Sciences 103 (2006) 8577.
[59] T. Richardson, P.J. Mucha, M.A. Porter, Physical Review E 80 (2009) 036111.
[60] V.D. Blondel, J.-L. Guillaume, R. Lambiotte, E. Lefebvre, Journal of Statistical Mechanics (2008) P10008.
[61] B.W. Kernighan, S. Lin, The Bell System Technical Journal 49 (1970) 291.
[62] B.H. Good, Y.-A. de Montjoye, A. Clauset, Physical Review E 81 (2010) 046106.
[63] S. Fortunato, M. Barthélemy, Proceedings of the National Academy of Sciences 104 (2007) 36.
[64] J. Reichardt, S. Bornholdt, Physical Review E 74 (2006) 016110.
[65] U. Brandes, D. Delling, M. Gaertler, R. Goerke, M. Hoefer, Z. Nikoloski, D. Wagner, IEEE Transactions on Knowledge and Data Engineering 20 (2008) 172.
[66] The use of resolution parameters to help identify communities that persist across a range of values is very useful for small networks such as the UNGA resolution networks but can be very problematic for larger systems because of the presence of numerous near-degeneracies in the modularity landscape [62], so the identification of appropriate resolution parameter values might be addressed statistically in such cases. See Ref. [13] for an illustration of this using protein-protein interaction networks.
[67] P. Bonacich, P. Lloyd, Social Networks 26 (2004) 331.
[68] M. Szell, R. Lambiotte, S. Thurner, Proceedings of the National Academy of Sciences 107 (2010) 13636.
[69] D. Cartwright, F. Harary, The Psychological Review 63 (1956) 277.
[70] M.J. Barber, Physical Review E 76 (2007) 066102.
[71] For clarity, we emphasize that we have repeated notation in the equations that define the modularity matrices corresponding to each network representation. This means that we have included symbols with different definitions in the different representations (e.g., m^+, k_i^+, and B_{ij}). The correct interpretation of the notation within each modularity-matrix definition is self-contained in the appropriate paragraphs of the above discussion.
[72] We identified G77-member countries using current G77 membership status. We did not take into account changes in membership over time.
[73] The Group of 77. 2009. Available at: http://www.g77.org/doc/members.html.
[74] J.-P. Onnela, D.J. Fenn, S. Reid, M.A. Porter, P.J. Mucha, M.D. Fricker, N.S. Jones, 2010. arXiv:1006.5731.
[75] M. Meilă, Journal of Multivariate Analysis 98 (2007) 873.
[76] B. Karrer, E. Levina, M.E.J. Newman, Physical Review E 77 (2008) 046119.
[77] R. Lambiotte, in: Proceedings of the 8th International Symposium on Modeling and Optimization in Mobile, Ad Hoc and Wireless Networks, WiOpt, 2010, p. 546.
[78] E. Voeten, A. Merdzanovic, 2009. Available at: http://hdl.handle.net/1902.1/12379.
[79] N.B. Weidmann, D. Kuse, K.S. Gleditsch, International Interactions 36 (2010) 86.